Eur. Phys. J. E (2012) **35**: 64
DOI 10.1140/epje/i2012-12064-3

THE EUROPEAN PHYSICAL JOURNAL E

Regular Article

Relaxation of the topological T1 process in a two-dimensional foam

P. Grassia[1,a], C. Oguey[2], and R. Satomi[1]

[1] CEAS, The Mill, University of Manchester, Oxford Rd, Manchester M13 9PL, UK
[2] LPTM, CNRS UMR 8089, University of Cergy-Pontoise, 2 ave A. Chauvin, 95302 Cergy-Pontoise, France

Received 7 March 2012 and Received in final form 10 May 2012
Published online: 26 July 2012 –

Abstract. The so-called topological T1 process, during which bubbles within a foam exchange neighbours is studied. The Durand and Stone model (Phys. Rev. Lett., **97**, 226101 (2006)) describes the growth of a film that is newly created during the T1 process, and also the evolution of surfactant concentration on this newly created film. Here some characteristic features of the Durand and Stone model (not previously described by Durand and Stone) are elucidated. In particular it is shown that the surfactant concentration on the newly created film is predicted to undergo an extremely rapid initial evolution, which occurs long before the film itself approaches anywhere near its final equilibrium length. Associated with this, the predicted length of the newly created film tends to exhibit an extremely rapid acceleration early on in its growth. An intermediate asymptotic analysis is developed to explain the above model predictions, by focussing on the regime when the film is several times larger than its initial length, but still several times smaller than its final length. A physical explanation is offered for these predictions in terms of slippage between material points instantaneously at the end of the newly created film, and the evolving location of the film endpoint itself: this slippage implies surfactant being transferred onto the newly created film from neighbouring films, overwhelming the amount of surfactant initially present. The implications of these predictions for the likely observations in an experimental study of the T1 process are discussed.

1 Introduction

Understanding transformations in bubble topology within a flowing foam is central to understanding foam rheology. Indeed the so-called topological T1 transformation, by which bubbles exchange neighbours is the key to plastic yielding behaviour of foam under imposed deformation [1–4].

In a fully 3-dimensional foam, there are various ways in which the T1 process might be realised. A film that separates two bubbles might disappear and be replaced by a new differently oriented film, or a film might be replaced by a new edge (at which three bubbles meet), or an edge might be replaced by a film [5].

The T1 process is simpler in a 2-dimensional foam, realised experimentally either as a raft of bubbles floating on liquid [6,7] (possibly with a confining upper plate [8]) or as a layer of bubbles confined between two plates [9]. In the 2-dimensional case [10], the T1 process can only involve a film disappearing and being replaced by another film roughly at right angles to the original one.

The newly created film is not at mechanical equilibrium, so must grow to approach equilibrium. The question then arises regarding the rate at which the newly created film grows, or in other words, regarding the inherent relaxation rate of the T1 process.

Indeed in a foam subjected to imposed shear, the overall rheological response will be quite different depending on whether the shear rate is smaller than the inherent relaxation rate (leading to quasistatic elastic deformation of foam punctuated by intermittent T1 processes [11,12]) or larger than the relaxation rate (continuous deformation [13]).

Surface rheological properties of the foam films (surface viscosity [14,15] and, in certain cases, Gibbs elasticity also [16,17]) are known to influence foam behaviour, and are expected to be important in controlling the T1 relaxation. Some years ago, Durand and Stone (hereafter DS) published a simple yet elegant model for describing the T1 relaxation process [18] and how it relates to surface rheological properties. The model treated both the evolution of the length of the newly created foam film, and the evolution of the concentration of surfactant on its surface. Although DS succeeded well in demonstrating that certain geometrical and kinematical observations from T1 relaxation experiments were consistent with their model, and although some special cases and/or simplified related models have been analysed subsequently [19], a detailed analysis of the full DS model predictions remains outstanding.

[a] e-mail: paul.grassia@manchester.ac.uk

The rate of (mechanical) relaxation after a T1, as predicted by the DS model, is one of a hierarchy of rates relevant to foam rheology. It has recently been pointed out that a physicochemical relaxation rate is also relevant [20,21], *i.e.* surfactant can take a finite time to reach the foam film surfaces. Indeed for certain surfactant types, the rate of physicochemical relaxation can even be *slower* than the mechanical relaxation rate [22]. In such a system, if the imposed shear rate is chosen on the same order as the physicochemical relaxation rate, the structure of the deforming foam can be computed as a mechanical equilibrium state, subject to the instantaneous (out-of-physicochemical-equilibrium) film surfactant coverages [20]. However, such computations exhibit discrete jumps at T1 topological transformations [21]: in fact topological transformation is necessarily an out-of-mechanical-equilibrium phenomenon and the aforementioned jumps can *only* be resolved by incorporating a viscous (or surface viscous) term such as the DS model contains. Thus, these recent studies of systems exhibiting slow physicochemical relaxation, far from drawing attention away from the (mechanical relaxation) DS model, have actually renewed interest in it.

In this study, a detailed analysis of the DS model will be performed. We will demonstrate that the DS model, despite its simplicity, actually contains an extremely rich physical behaviour. Specifically we will show:

1) The DS model predicts an extremely rapid initial evolution for surfactant concentration on the newly created film surface (concentration changes significantly even whilst the newly created film is a tiny fraction of the length of any neighbouring films) followed by a much more gradual evolution in surfactant concentration thereafter.
2) Although the length of the newly created film *vs.* time decelerates on the approach to a final steady state length (as one would expect), the film length predicted by the DS model actually exhibits a dramatic acceleration in the early stages of its growth.

The remainder of this study is laid out as follows. In sect. 2 we review the DS model. One key finding will be that the DS model admits (in principle) two regimes of final steady state behaviour following a T1, one in which the final length of the newly created film is close to its initial length, and the other in which the final length is orders of magnitude larger than the initial length. The latter situation however turns out to be the physically realistic one. Accordingly in sect. 3 we compute the final steady state length of the newly created film (far from its initial length), and also the approach to this steady state. In sect. 4 we consider instead an "intermediate" regime, in which the length of the newly created film is significantly greater than its initial value, but much smaller than its final value: consideration of this intermediate regime is essential to understand the dramatic accelerations in film length which were mentioned above. Finally in sect. 5 we give a summary and conclusions.

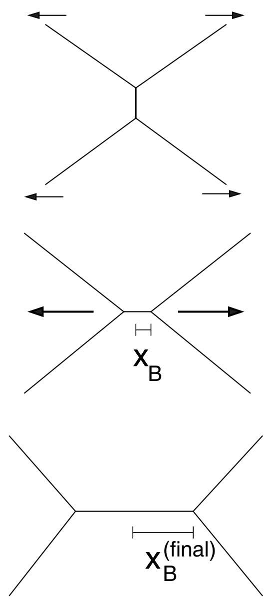

Fig. 1. Geometrical situation considered in the DS model: due to some imposed deformation (upper figure), a film disappears and is replaced (middle figure) by a reoriented, newly created film, which then grows over time towards a final equilibrium value (lower figure), whilst its neighbours shrink. The time evolution of the length $2x_B$ of the growing film is of interest.

2 Durand and Stone (DS) model

Here we develop the DS model in three parts: the geometry of the DS model (sect. 2.1), the surfactant mass balance in the DS model (sect. 2.2), and the vertex evolution of the DS model (sect. 2.3). For full details of the derivation of the model, see [18].

2.1 Model geometry

The geometrical situation that DS considered is sketched in fig. 1.

Five films participate directly in the T1 relaxation process, the newly created film (hereafter the growing film) and the four films to which it is attached (hereafter the shrinking films).

The origin of a coordinate system is placed at the centre of the growing film, a coordinate axis being aligned with the film itself.

By symmetry, it is sufficient to consider a quadrant (as in fig. 2) formed by half of the growing film, plus one of the shrinking films, the quadrant being assumed to enclose an area L_x by L_y.

The objective is to compute the vertex position (denoted x_B) as a function of time t, the evolution of the shrinking film length (denoted L) then following from geometry

$$L = \sqrt{L_y^2 + (L_x - x_B)^2}. \qquad (1)$$

At the instant of T1, x_B is assumed to be created with some known value x_0, which is related to the liquid fraction in the foam. It is assumed that $x_0 \ll \sqrt{L_x^2 + L_y^2}$, *i.e.*

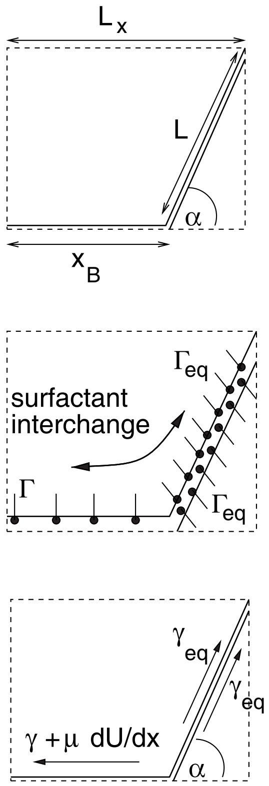

Fig. 2. Quadrant considered in the DS model. Upper figure: geometry of the quadrant; middle figure: surfactant interchange within the quadrant; lower figure: force balance on the quadrant.

the growing film is initially much shorter than its neighbours. Generally it is not possible to realise this condition in the case of wet foam, *e.g.* a layer of bubbles floating on liquid [6–8], but the condition can be realised for a dry foam, *e.g.* a bubble layer confined between two plates [9], so this latter system is the case considered here.

Moreover it is assumed that $L_x = \sqrt{3}L_y$, from which it is evident that, in the initial configuration, films at the threefold vertex meet at angles far from $\frac{2\pi}{3}$, and the system is far from mechanical equilibrium. In fact under these conditions the angle α between the shrinking film and the horizontal axis, defined such that

$$\cos\alpha \equiv (L_x - x_B)/L, \tag{2}$$

is actually initially very close to $\frac{\pi}{6}$.

2.2 Surfactant mass balance

In addition to considering the geometry of the T1 process, the DS model also concerns itself with surfactant balance on film surfaces.

Initially all surfaces are assumed to be created with some (physicochemical) equilibrium surfactant surface concentration $\Gamma_{\rm eq}$, taken to have units of amount of surfactant per length in a 2-dimensional representation of the films. This assumption implies that the shear rate imposed to induce the T1 transformation is considerably smaller than the system's inherent physicochemical relaxation rate: otherwise surface concentrations would necessarily depart from equilibrium even in the initial state as the T1 commences.

Subsequently DS assume that surfactant is able to move along film surfaces, but not (on the timescales of interest) to migrate across the film thickness: exchange of surfactant between the surfaces of films and their bulk is therefore neglected in the DS model. Thus in a quadrant as shown in fig. 2, the total amount of surfactant on one surface of the growing film plus that on one surface of the shrinking film is assumed to be conserved. This conserved constant is necessarily equal to $\Gamma_{\rm eq}L_c$, where

$$L_c = \sqrt{L_y^2 + (L_x - x_0)^2} + x_0. \tag{3}$$

Notice that a minimal value of L_c (denoted $L_c^{\min}$) is only realised in the limit $x_0 \to 0$.

DS make the further assumption that the concentration only on the growing film (denoted Γ) evolves, whereas that on the shrinking film remains constant at the value $\Gamma_{\rm eq}$. It then follows from surfactant conservation that

$$\Gamma/\Gamma_{\rm eq} = (L_c - L)/x_B, \tag{4}$$

so that the instantaneous surfactant coverage can be deduced entirely via the geometry. Equation (4) also implies a very specific level of surfactant transport from film to film: the cumulative surfactant transported onto the growing film is in fact $\Gamma x_B - \Gamma_{\rm eq}x_0 = \Gamma_{\rm eq}(L_c - L - x_0)$.

It is eq. (4) which leads to one of the features of the DS model, namely that $\Gamma/\Gamma_{\rm eq}$ evolves extremely rapidly initially, changing significantly long before the growing film has acquired significant length compared to the shrinking films.

To explain how such a situation comes about, we consider units for which $L_x = 3/4$ and $L_y = \sqrt{3}/4$, so that the limit $x_B \to x_0 \ll 1$ corresponds to $\alpha \approx \frac{\pi}{6}$ and $x_B \to \frac{1}{2}$ corresponds to $\alpha = \frac{\pi}{3}$.

We then note that, provided $x_0 \le x_B \ll 1$, the values of L_c and L are close to one another, and eq. (4) represents a ratio of two small quantities. Such a quotient is very susceptible to changes as either the numerator or the denominator or both are changed.

Specifically if L_c and L are Taylor expanded in x_0 and x_B, respectively, we find that

$$\frac{\Gamma}{\Gamma_{\rm eq}} \approx \frac{\sqrt{3}}{2} + \left(1 - \frac{\sqrt{3}}{2}\right)\frac{x_0}{x_B} \quad \text{provided} \quad x_0 \le x_B \ll 1. \tag{5}$$

Thus $\Gamma/\Gamma_{\rm eq}$ can fall from unity to $\frac{\sqrt{3}}{2}$ even whilst $x_B \ll 1$.

Once $x_B \gg x_0$, it would be permitted to replace L_c by $L_c^{\min}$ in eq. (4) to yield

$$\Gamma/\Gamma_{\rm eq} \approx (L_c^{\min} - L)/x_B \quad \text{provided} \quad x_0 \ll x_B. \tag{6}$$

This gives a value which decreases gradually from $\frac{\sqrt{3}}{2}$ when $x_B \ll 1$ to $\sqrt{3} - 1$ as $x_B \to \frac{1}{2}$.

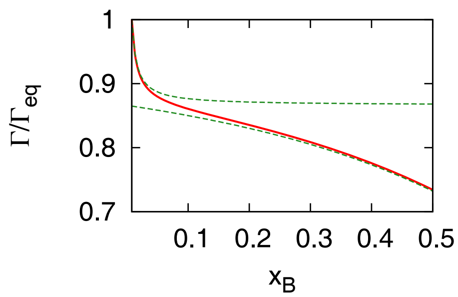

Fig. 3. Graph of $\Gamma/\Gamma_{\rm eq}$ *vs.* x_B (solid curve). Two asymptotic formulae (dashed curves): one valid for $x_B \ll 1$ and the other valid for $x_B \gg x_0$ are also shown. The value $x_0 = \frac{1}{128}$ was used here.

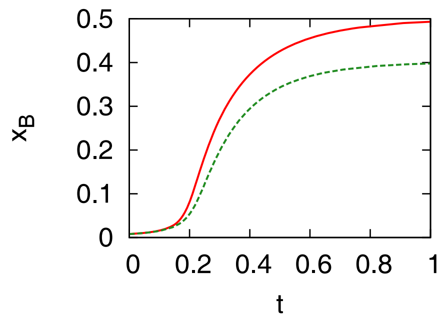

Fig. 4. Numerical solutions x_B *vs.* t for the DS model (all quantities are in dimensionless form). Upper curve is for $\epsilon/\gamma_{\rm eq} = 0$ and lower curve is for $\epsilon/\gamma_{\rm eq} = 1$. The value $x_0 = \frac{1}{128}$ was used here.

A graph of $\Gamma/\Gamma_{\rm eq}$ *vs.* x_B (eq. (4) for the value $x_0 = \frac{1}{128}$) is plotted in fig. 3 alongside the two asymptotic formulae (5) and (6).

This figure makes it clear that, as x_B grows, there is a rapid initial change in $\Gamma/\Gamma_{\rm eq}$, whilst subsequent changes are slower. This behaviour —and especially the particular value of $\Gamma/\Gamma_{\rm eq}$ attained by the end of the rapid initial change— turns out to have important implications for the evolution of x_B *vs.* t, a point we will return to later.

2.3 Vertex evolution

As well as considering surfactant transport, the DS model also computes the temporal evolution of vertex position x_B, during mechanical relaxation following a T1. Those endpoints of the shrinking films not connected to the growing film (see fig. 1) are assumed fixed in position during the relaxation evolution, which again implies that the shear rate imposed to induce the T1 is considerably smaller than the system's inherent mechanical relaxation rate. Determining the vertex evolution in the DS model begins by considering a force balance (see fig. 2) in each quadrant between both surfaces of a shrinking film (angled at α from the horizontal and each assumed to maintain a constant surface tension $\gamma_{\rm eq}$) and one surface of the growing film (with a variable surface tension γ that depends on the instantaneous surfactant concentration Γ via an equation of state $\gamma = \gamma_{\rm eq} - \epsilon \log(\Gamma/\Gamma_{\rm eq})$) plus a surface viscosity term on the growing film (that depends on a surface viscosity μ and the extension rate of surface fluid elements $\partial U/\partial x$). Thus

$$2\gamma_{\rm eq}\cos\alpha - \gamma - \mu\frac{\partial U}{\partial x}$$
$$= 2\gamma_{\rm eq}\cos\alpha - \gamma_{\rm eq} + \epsilon\log\left(\frac{\Gamma}{\Gamma_{\rm eq}}\right) - \mu\frac{\partial U}{\partial x} = 0. \qquad (7)$$

The DS model recognises that $\partial U/\partial x$ is not equal to $\dot{x}_B/x_B$ because fluid elements transfer between films, so there is no requirement for fluid element stretch in the growing film to keep pace with vertex motion.

Fluid element stretch can however be related to surfactant coverage evolution via a surfactant conservation equation

$$\partial U/\partial x = -\dot{\Gamma}/\Gamma. \qquad (8)$$

Remember that surfactant coverage can be related entirely geometrically to vertex position via eq. (4), so that differentiating this equation with respect to time, recognising also that $\dot{L} = -\dot{x}_B\cos\alpha$, a relation between $\dot{x}_B/x_B$ and $\partial U/\partial x$ follows. Specifically

$$\frac{\partial U}{\partial x} = \left(1 - \frac{\cos\alpha}{\Gamma/\Gamma_{\rm eq}}\right)\frac{\dot{x}_B}{x_B} = \left(1 - \frac{x_B\cos\alpha}{(L_c - L)}\right)\frac{\dot{x}_B}{x_B}. \qquad (9)$$

Substitution of eq. (9) in eq. (7) produces an evolution equation for $\dot{x}_B$, which can be easily solved numerically. Some typical solutions are plotted in fig. 4.

Equation (9) indicates some potentially extremely interesting behaviour for $\dot{x}_B/x_B$ when the value of x_B satisfies $x_0 \ll x_B \ll 1$. In that case both $\cos\alpha$ and (via eq. (5)) $\Gamma/\Gamma_{\rm eq}$ will be close to $\frac{\sqrt{3}}{2}$. Thus via eq. (9), $\dot{x}_B/x_B$ will become much larger than $\partial U/\partial x$, indicating a dramatic acceleration[1] in the length of the growing film in the domain $x_0 \ll x_B \ll 1$. We will return to this point later in sect. 4. Before doing that, however, we will consider the final state of the DS model.

3 Final state of the DS model

The DS model eventually achieves a final steady state value of x_B, denoted $x_B^{\rm final}$ for which the surface viscosity term in eq. (7) vanishes.

Note that, owing to the assumption that the shrinking film tension is fixed at $\gamma_{\rm eq}$, there is no requirement to impose equal film tensions in the final state[2] and thus no requirement for films to meet at $\frac{2\pi}{3}$ angles, a point which is discussed further in appendix A. Indeed equal tensions

[1] Inertial effects are ignored in the DS model, and will not be considered here. However inertia would be expected to moderate these predicted dramatic accelerations.

[2] Physically the tensions must eventually become equal, but that involves surfactant transport processes— *i.e.* surfactant exchange between film surface and bulk —occurring on time scales longer than those of interest for the DS model.

in the final state are only realised in the limit $\epsilon \to 0$ (the so called Plateau case, as considered by [19]).

There is an interesting question regarding whether, in the DS model, it is ever possible to find a value of x_B^{final} in the neighbourhood of the initial vertex position $x_0 \ll 1$, or whether the final state is necessarily shifted significantly away from the initial state. In other words, is the growing film ever sufficiently elastic that even a small change in its length is sufficient to balance the net pull from the surrounding shrinking films?

It turns out that for all practical purposes this cannot be achieved. It would require a value of $\epsilon/\gamma_{\mathrm{eq}}$ at least $(\sqrt{3}-1)/\log(2/\sqrt{3}) \approx 5.08$ which is bigger than observed in practice (DS [18] reported experimental $\epsilon/\gamma_{\mathrm{eq}}$ values of 0.8 or 1.2 depending on their surfactant system).

Note that a recent study [21] predicted cases with $x_B^{\mathrm{final}} \ll 1$ for a much smaller value $\epsilon/\gamma_{\mathrm{eq}} = \sqrt{3}-1$. This, however, assumed surfactant to be conserved on the growing film, making the growing film much stiffer than in the DS model, where it can receive additional surfactant from the neighbouring shrinking films. The recent study [21] alluded to above, also linearized the equation of state to $\gamma = \gamma_{\mathrm{eq}} - \epsilon(-1 + \Gamma/\Gamma_{\mathrm{eq}})$ but linearising the isotherm makes no material difference in the DS predictions. A linearised isotherm in the DS model would have required $\epsilon/\gamma_{\mathrm{eq}}$ at least $(\sqrt{3}-1)/(1-\sqrt{3}/2) \approx 5.46$ to have $x_B^{\mathrm{final}} \ll 1$, but again values of $\epsilon/\gamma_{\mathrm{eq}}$ this large are not observed in practice. Thus for practical purposes x_B^{final} is a value much larger than x_0 and consequently is very insensitive to whichever x_0 value (provided $x_0 \ll 1$) is chosen.

The question then arises regarding the value of x_B^{final} as a function of $\epsilon/\gamma_{\mathrm{eq}}$. This can be determined by setting $\partial U/\partial x$ to zero in eq. (7), and substituting for Γ from eq. (4) to deduce

$$\frac{(2\cos(\alpha(x_B^{\mathrm{final}}))-1)}{\log(x_B^{\mathrm{final}}/(L_c^{\mathrm{min}} - L(x_B^{\mathrm{final}})))} = \epsilon/\gamma_{\mathrm{eq}}, \qquad (10)$$

a nonlinear equation which needs to be solved for x_B^{final} given $\epsilon/\gamma_{\mathrm{eq}}$.

The resulting x_B^{final} computed via a Newton-Raphson procedure turns out to be remarkably close to a straight line function of the parameter $\epsilon/\gamma_{\mathrm{eq}}$ —see fig. 5: the deviation from the straight line in the computed x_B^{final} is extremely small, a result which follows because the left hand side of eq. (10) happens to be a very nearly a straight line function of its argument. Thus to an excellent approximation, in the DS model

$$x_B^{\mathrm{final}} \approx \frac{1}{2}\left(1 - \frac{\epsilon}{5.08\gamma_{\mathrm{eq}}}\right). \qquad (11)$$

For comparison, final x_B values (as a function of $\epsilon/\gamma_{\mathrm{eq}}$, and assuming the case of no surfactant transfer onto the growing film) have also been indicated on fig. 5: these are much smaller than the DS model x_B^{final} predictions. Evidently surfactant transfer from the shrinking films to the growing film (as permitted by the DS model) is a significant factor in determining x_B^{final}.

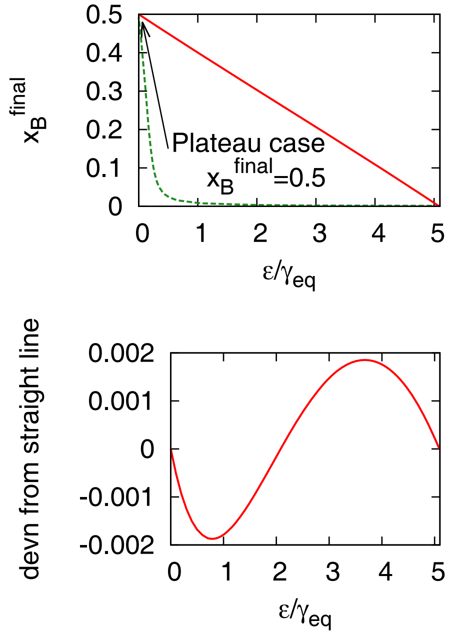

Fig. 5. Upper figure: the final state x_B^{final} (solid line) of the DS model *vs.* the Gibbs elasticity parameter $\epsilon/\gamma_{\mathrm{eq}}$, contrasted with an alternative model (dashed curve) whereby the growing film is not permitted to receive surfactant from its neighbours. Lower figure: the deviation of the DS model x_B^{final} from the straight line approximation of eq. (11).

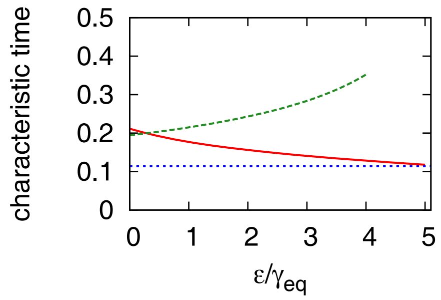

Fig. 6. Characteristic times, one associated with approach to the final steady state (solid curve; see sect. 3.1), one associated with the time to transit to the neigbourhood of the final steady state (dotted line, independent of $\epsilon/\gamma_{\mathrm{eq}}$; see sect. 4.3) and another being the initial delay time before achieving significant film growth rates (dashed curve; see eq. (23)), plotted *vs.* $\epsilon/\gamma_{\mathrm{eq}}$. Data for delay time are not presented for large $\epsilon/\gamma_{\mathrm{eq}}$, because significant film growth never occurs in that particular regime.

3.1 Approach to steady state

Having determined the final steady state value x_B^{final} as a function of $\epsilon/\gamma_{\mathrm{eq}}$, it is worthwhile considering the rate of approach to this final mechanical equilibrium state. DS have pointed out that the relevant rate should be γ_{eq}/μ multiplied by a dimensionless function of $\epsilon/\gamma_{\mathrm{eq}}$: they did not however determine the dimensionless function.

By linearising the evolution equation for x_B about x_B^{final}, we have demonstrated that x_B has an exponential approach to $x_B^{\rm final}$ with a characteristic approach time (the reciprocal of the rate constant) as shown in fig. 6: the approach time is a decreasing function of $\epsilon/\gamma_{\rm eq}$. This does not however fully answer how the overall x_B *vs.* t evolution depends on $\epsilon/\gamma_{\rm eq}$ because it concerns a purely local analysis in the neighbourhood of $x_B^{\rm final}$. Only by also considering values away from $x_B^{\rm final}$ can a more global picture of the temporal evolution be obtained, a topic to which we return in sect. 4 below.

4 Intermediate regime: $x_0 \ll x_B \ll x_B^{\rm final}$

For a dry foam, new films are created with lengths initially much smaller than the lengths of their neighbours, *i.e.* $x_0 \ll 1$ in our dimensionless system. Meanwhile we have seen that final film lengths $x_B^{\rm final}$ are much larger than x_0, and moreover are quite insensitive to the precise value of x_0, but instead depend primarily on $\epsilon/\gamma_{\rm eq}$. This indicates that at some stage during its temporal evolution x_B will pass through an "intermediate" regime for a period of time during which $x_0 \ll x_B$ but also $x_B \ll x_B^{\rm final}$.

The DS model x_B actually exhibits an extremely interesting temporal evolution in this "intermediate" regime, a point we now discuss. In particular, in sect. 4.1, the equations governing the intermediate regime are derived. These are then analysed in three distinct subregimes (sects. 4.2–4.4) all falling within the intermediate regime. Next a physical interpretation of particular subregime behaviour is offered in sect. 4.5. An interpolation spanning all three subregimes is introduced in sect. 4.6 with an important consequence of the interpolation formula being discussed in sect. 4.7. Finally sect. 4.8 considers how well the intermediate regime formulae match to full DS model solutions beyond the intermediate regime.

4.1 Governing equations of the intermediate regime

In the intermediate regime, eq. (9) can be replaced by

$$\frac{\partial U}{\partial x} = \left(\left(\frac{2}{\sqrt{3}} - 1 \right) \frac{x_0}{x_B} + \frac{1}{6} x_B \right) \frac{\dot{x}_B}{x_B}. \qquad (12)$$

The factor in parentheses on the right hand side of (12) has been determined by combining eq. (5) with Taylor expansions of (2) and (6). For reasons to be made apparent later, we shall refer to this factor as a "slip coefficient".

The governing equation for $\dot{x}_B$ in the intermediate regime becomes (adopting units for which both $\gamma_{\rm eq}$ and μ reduce to unity)

$$\left(\sqrt{3}-1\right) - \epsilon \log\left(\frac{2}{\sqrt{3}}\right) = \left(\left(\frac{2}{\sqrt{3}} - 1 \right) \frac{x_0}{x_B} + \frac{1}{6} x_B \right) \frac{\dot{x}_B}{x_B} \quad \text{for} \quad x_0 \ll x_B \ll x_B^{\rm final}. \qquad (13)$$

Bearing in mind the near linearity of $x_B^{\rm final}$ with ϵ observed in fig. 4, we can actually approximate eq. (13) extremely well by

$$2(\sqrt{3}-1) x_B^{\rm final} = \left(\left(\frac{2}{\sqrt{3}} - 1 \right) \frac{x_0}{x_B} + \frac{1}{6} x_B \right) \frac{\dot{x}_B}{x_B}. \qquad (14)$$

This equation actually applies throughout the domain $x_0 \ll x_B \ll x_B^{\rm final}$, but simplifies further according to whether $x_B \ll x_0^{1/2}$ or $x_B \gg x_0^{1/2}$. Remember that over time, x_B evolves from an initial value x_0 (with $x_0 \ll 1$ for the case of a dry foam as we consider here) to a final value (see sect. 3) of order unity. Thus whether $x_B \ll x_0^{1/2}$ or $x_B \gg x_0^{1/2}$ depends on how far along in its temporal evolution the system is at any particular instant. We now proceed to consider these limits/subregimes.

4.2 The subregime $x_B \ll x_0^{1/2}$

In the case $x_B \ll x_0^{1/2}$ we obtain

$$\dot{x}_B \approx \frac{2(\sqrt{3}-1)}{\left(\frac{2}{\sqrt{3}} - 1\right)} \frac{x_B^{\rm final}}{x_0} x_B^2 \approx 9.46 \frac{x_B^{\rm final}}{x_0} x_B^2, \qquad (15)$$

which exhibits super-exponential growth

$$x_B \approx \left(\frac{1}{x_{B0}} - 9.46 \frac{x_B^{\rm final}}{x_0} (t - t_0) \right)^{-1}. \qquad (16)$$

Here x_{B0} is an arbitrarily chosen value selected such that $x_0 \ll x_{B0} < O(x_0^{1/2})$ and t_0 is the time (determined *e.g.* via numerical integration of the full evolution equation) at which $x_B = x_{B0}$. Different choices of the parameter x_{B0} would require different t_0 values, but do so in such a way that the x_B *vs.* t formula (16) remains insensitive to the precise choice of x_{B0}.

The reason we are obliged to parameterise (16) in this way is that intermediate regime equation (13) does not apply all the way down to $t = 0$ with $x_B \to x_0$. The expression for the "slip coefficient" on the right hand side of eq. (13) and/or (14) becomes more complicated in the limit $x_0/x_B \to 1$. Additionally, in this same limit, there is variation in the tension contribution from Gibbs elasticity which is more complicated than the left hand side of eq. (13) suggests.

Regardless of which x_{B0} and t_0 values we utilise, eq. (16) predicts x_B diverging in finite time. Such a divergence is of course unphysical, because once x_B grows to become $O(x_0^{1/2})$ or greater, eq. (15) ceases to apply, and we must return to consider eqs. (13) or (14).

4.3 The subregime $x_B \gg x_0^{1/2}$

For $x_B \gg x_0^{1/2}$, we find via eq. (14) that $\dot{x}_B$ saturates at a maximum value that we denote $\dot{x}_B^{\rm sat}$

$$\dot{x}_B^{\rm sat} \approx 12(\sqrt{3}-1) x_B^{\rm final} \approx 8.78 x_B^{\rm final}. \qquad (17)$$

Equation (17) can be used for estimating time scales for system evolution. Recall that in sect. 3.1 we plotted the characteristic time required to approach to a final equilibrium state, based solely on a local analysis in the neighbourhood of $x_B^{\rm final}$. Such an analysis however did not answer the question of how long it takes to arrive at the

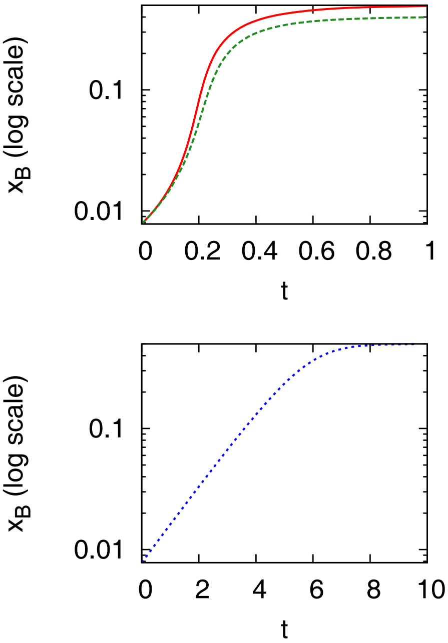

Fig. 7. Upper figure: numerical solutions x_B *vs.* t on the domain $0 \leq t \leq 1$ for the DS model (cf. fig. 4) plotted on log-linear axes (all quantities are in dimensionless form). The solid curve is for $\epsilon/\gamma_{\rm eq} = 0$ and the dashed curve is for $\epsilon/\gamma_{\rm eq} = 1$. Lower figure: numerical solutions x_B *vs.* t on the domain $0 \leq t \leq 10$ predicted by the model of Biance and co-workers [19] using the same parameter value $\epsilon/\gamma_{\rm eq} = 0$ as in that reference.

neighbourhood of $x_B^{\rm final}$. Estimating the time required for this as $x_B^{\rm final}/\dot{x}_B^{\rm sat}$ yields a value $1/(12(\sqrt{3}-1)) \approx 0.114$, independent of $x_B^{\rm final}$ *i.e.* independent of ϵ. This time estimate is indicated on fig. 6 where it can be compared with the estimates computed from the local near-equilibrium analysis.

4.4 Values of x_B in the neighbourhood of $x_0^{1/2}$

To date we have considered eq. (14) only in the simplifying limiting cases $x_B \ll x_0^{1/2}$ or $x_B \gg x_0^{1/2}$.

When instead $x_B = O(x_0^{1/2})$, eq. (14) indicates that $\dot{x}_B/x_B$ has a maximum when

$$x_B = x_B^{\rm infl} \equiv \left(6\left(\frac{2}{\sqrt{3}}-1\right)\right)^{1/2} x_0^{1/2} \approx 0.963 x_0^{1/2}. \quad (18)$$

This means that a graph of $\log(x_B)$ *vs.* t exhibits an inflection point: figure 7 shows that this is indeed the case.

Comparing fig. 4 and fig. 7 we see that the DS model exhibits an inflection point both in graphs of x_B *vs.* t and $\log x_B$ *vs.* t. Inflection points in fig. 4 are unsurprising and would be predicted by other models for the T1 process *e.g.* that of Biance and co-workers [19] which assumes[3] $\partial U/\partial x = \dot{x}_B/x_B$. This particular type of inflection arises because some acceleration of x_B is expected at early times as, in the presence of surface viscosity, it becomes easier to sustain velocity differences over a longer film than over a short one. Meanwhile x_B must decelerate on the approach to a final steady state where the net pull on the vertex becomes zero.

Inflections in fig. 7 are however a characteristic feature of the DS model, not predicted by the model[4] of Biance and co-workers [19]: the accelerations of x_B predicted by DS are therefore far more dramatic than those seen by Biance and co-workers. The physical implications of these DS model specific inflections are now considered.

4.5 Interpretation of inflections in $\log x_B$ vs. t

In the DS model, the vertex velocity, $\dot{x}_B$, slips with respect to that of material points[5] at the vertex, $x_B\, \partial U/\partial x$. It is clear from the definitions in sect. 2.3 that slippage occurs whenever the aforementioned "slip coefficient" (as defined in the discussion following eq. (12)) differs from unity. This indicates that surfactant is being transferred from one film to another, and indeed, in the neighbourhood of the inflection, where the slip coefficient is a minimum with a value much smaller than unity, the relative slip between the vertex itself and the material points is very large.

The physics described by the DS model can be explained with the aid of a sketch: see fig. 8. The model describes a stretching operation which occurs in parallel with a cut-stretch-paste. During a time $\mathrm{d}t$ stretching moves a material point on the growing film from a position x_B to $x_B + \mathrm{d}t\, x_B\, \partial U/\partial x$. Meanwhile a segment $\mathrm{d}x_B \cos\alpha$ of the shrinking film is cut from that film, stretched by a factor $\Gamma_{\rm eq}/\Gamma$ (to ensure its surfactant coverage matches that of the growing film) and is pasted onto the growing film. The net growth $\mathrm{d}x_B$ therefore is

$$\mathrm{d}x_B = \mathrm{d}t\, x_B \frac{\partial U}{\partial x} + \mathrm{d}x_B \frac{\cos\alpha}{\Gamma/\Gamma_{\rm eq}}, \quad (19)$$

which corresponds exactly to eq. (9).

Should $(\cos\alpha)/(\Gamma/\Gamma_{\rm eq})$ ever become close to unity, as indeed it does in the neighbourhood of the inflection,

[3] Whilst Biance *et al.* [19] formulated their model such that $\partial U/\partial x = \dot{x}_B/x_B$, their formulation could have equally well assumed $\partial U/\partial x = \beta \dot{x}_B/x_B$, where β is some constant: one requires $\beta < 1$ in order for surfactant to be transported from shrinking films to the growing film, and indeed fixing β specifies precisely how much surfactant transfers. Discrepancies that Biance *et al.* report between the time scales of their model predictions and their experimental results (and which they speculate may be due to 3-dimensional effects in their experiments), could have been explained simply by setting $\beta = 0.4$.

[4] Note that [19] chose the value $\epsilon/\gamma_{\rm eq} = 0$ based on experimental data for their system. When the growing film is not permitted to exchange surfactant with its neighbours, it would stiffen considerably as it grows at any finite $\epsilon/\gamma_{\rm eq}$, limiting the final length it can attain (see also fig. 5). At $\epsilon/\gamma_{\rm eq} = 1$, the model of [19] leads to tiny $x_B^{\rm final}$ values, $x_B^{\rm final} \ll 1$, so x_B *vs.* t data for this particular case are not considered in fig. 7.

[5] The concept of film material points tied to surfactant molecules is explained in [23].

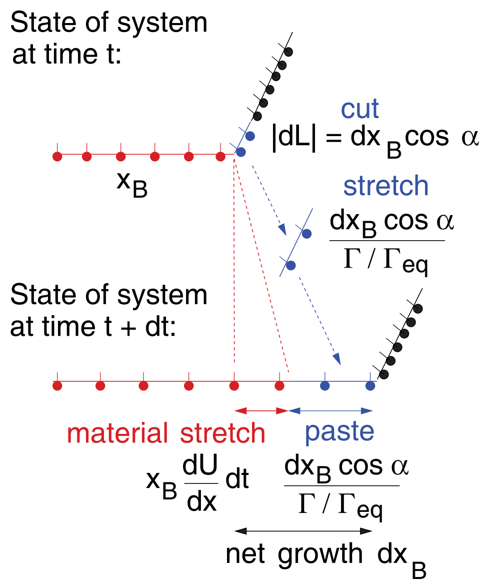

Fig. 8. The growth of x_B in the DS model viewed as a combination of a stretch operation (on the growing film) and a cut-stretch-paste operation (from the shrinking film to the growing film).

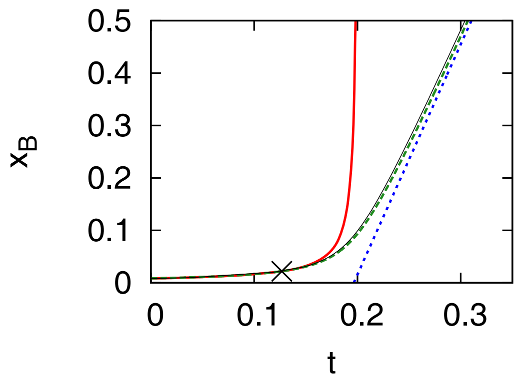

Fig. 9. Intermediate regime solutions for x_B *vs.* t (in dimensionless form) in the case $\epsilon/\gamma_{\rm eq} = 0$ (data for other cases *e.g.* $\epsilon/\gamma_{\rm eq} = 1$, although not shown here, exhibit similar qualitative behaviour). The super-exponential growth formula eq. (16) (solid line), the intermediate regime formula being the solution to eq. (20) (dashed line), the straight line saturation formula eq. (21) (dotted line). The value of (t_0, x_{B0}) used to "anchor" the above solutions is marked by $\times$: we chose $x_{B0} = \frac{1}{4}x_0^{1/2}$ with $x_0 = \frac{1}{128}$ for the purposes of this figure. The numerical solution used to obtain the (t_0, x_{B0}) value is also shown (thin line).

film growth is completely dominated by the cut-stretch-paste operation, and exceedingly large $\dot{x}_B$ values result via eq. (9), despite a finite $\partial U/\partial x$. This is what produces the dramatic acceleration in film length x_B in the DS model. Indeed there are very striking differences in the DS predictions which permit "slippage" between $\dot{x}_B/x_B$ and $\partial U/\partial x$ via equation (9), and those of the model formulated by Biance and co-workers [19] which constrains $\dot{x}_B/x_B$ to equal $\partial U/\partial x$. No dramatic acceleration for x_B is predicted in the latter model, making the overall film length evolution much slower: see fig. 7.

4.6 Interpolating between the limits $x_B \ll x_0^{1/2}$ and $x_B \gg x_0^{1/2}$

It is possible to find a solution of eq. (14) which interpolates between the super-exponential growth characteristic of $x_B \ll x_0^{1/2}$ and the saturated film growth rate observed for $x_B \gg x_0^{1/2}$, incorporating the regime $x_B = O(x_0^{1/2})$ in between.

For convenience in what follows we will denote the constant $(x_B^{\rm infl}/\, x_0^{1/2})^2 \equiv 6(\frac{2}{\sqrt{3}} - 1) \approx 0.928$ by the symbol χ.

Then we can write (14) in the equivalent form

$$\dot{x}_B^{\rm sat} = \left(\frac{\chi x_0}{x_B} + x_B\right)\frac{\dot{x}_B}{x_B}\,. \tag{20}$$

The solution proceeds by integrating both sides of eq. (20) to find t as a function of x_B, and then solving a quadratic to obtain x_B explicitly in terms of t. As before we must parameterise the solution in terms of an arbitrarily chosen x_{B0} value, and the t_0 value (found *e.g.* numerically —or else via the approximate theory sketched out in appendix B) that corresponds to the chosen x_{B0}. The resulting x_B *vs.* t is however insensitive to the choice of x_{B0} provided $x_0 \ll x_{B0} \ll x_B^{\rm final}$.

The resulting x_B *vs.* t is plotted in fig. 9 where it is compared[6] against the super-exponential solution (16). Also plotted on this figure is a numerical solution obtained from a generalisation of eq. (13) which assumes $x_B \ll 1$, but which permits x_0/x_B to be any value up to unity. Both the Gibbs elasticity term on the left of the governing equation and the slip coefficient on the right differ from what is shown in eq. (13) in this case. This numerical solution also conveniently provides the data point $(t, x_B) = (t_0, x_{B0})$ used to fix the solution to eq. (20), and indeed the two solutions are close throughout the full range of t and x_B considered, not merely in the neighbourhood of (t_0, x_{B0}).

For large values of $t - t_0$ the solution to (20) approaches a straight line (also plotted on fig. 9)

$$x_B \approx -\chi\frac{x_0}{x_{B0}} + x_{B0} + \dot{x}_B^{\rm sat}(t - t_0), \tag{21}$$

where x_{B0} and t_0 have their former meanings, except that now we permit x_{B0} values up to and including $O(x_0^{1/2})$.

Unsurprisingly (in view of the discussion in sect. 4.3) the slope of this line is $\dot{x}_B^{\rm sat}$. However eq. (21) provides additional information, namely an intercept. We write eq. (21) in the form

$$x_B \approx \dot{x}_B^{\rm sat}(t - t_{\rm delay}), \tag{22}$$

[6] In order to show more clearly how the intermediate solution evolves, it has been convenient to plot all the way up $x_B = 0.5$ here. This is of course well outside the regime of applicability of the intermediate solution: see sect. 4.8 for details of matching with solutions outside this regime.

where t_{delay} is an apparent delay time, defined as

$$t_{\text{delay}} = t_0 - \frac{x_{B0}}{\dot{x}_B^{\text{sat}}} + \frac{\chi x_0}{\dot{x}_B^{\text{sat}} x_{B0}}\,. \tag{23}$$

Different values of x_{B0} require different t_0 as we have said, but do so in such a way that t_{delay} remains insensitive to the precise choice of x_{B0}.

4.7 The apparent delay time t_{delay}

The significance of the apparent delay time is as follows.

According to the DS model, initially x_B grows quite slowly, it then accelerates (and $\dot{x}_B$ saturates at the value $\dot{x}_B^{\text{sat}}$ when $x_0^{1/2} \ll x_B \ll x_B^{\text{final}}$), and finally x_B decelerates on the approach to a final steady state.

Owing to the fact that the saturation velocity is attained even whilst x_B is very small, it can be quite difficult experimentally to resolve the initial film growth and acceleration dynamics. Experimental data in the subsequent saturation and deceleration regimes are far easier to obtain (and indeed this is all that DS reported [18]).

Experimentally in a real foam at finite liquid fraction the time at which a T1 event begins is not known precisely: one is required to make a difficult judgement regarding precisely when finite size Plateau borders separate to produce a new film. If one is not anticipating any particularly complex dynamics for x_B at early times, it is natural to extrapolate the experimentally observed x_B *vs.* t data down to $x_B = 0$ in an effort to estimate when the T1 event began. However, if one extrapolates the straight line solution (21) or (22) down to $x_B = 0$, one obtains a time $t = t_{\text{delay}}$. Even though the T1 really began at time $t = 0$, it may appear to have begun at $t = t_{\text{delay}}$, since growth was comparatively slow up until that point.

We have computed the value of this delay time, as a function of ϵ. We selected $x_{B0} = x_0^{1/2}$ for these computations[7], but checked that the results were insensitive to values of x_{B0} between $\frac{1}{4}x_0^{1/2}$ and $2x_0^{1/2}$. Keeping $x_{B0} = x_0^{1/2}$, we also checked that t_{delay} was quite insensitive to the value of x_0, which was varied by a factor of four: fig. 6 corresponds to $x_0 = \frac{1}{128}$. In fig. 6, when computing t_{delay}, we also restrict the range of ϵ values considered (excessively large ϵ values are avoided) to ensure that x_B^{final} remains greater than our chosen x_{B0}.

Figure 6 shows that the delay time t_{delay} is an increasing function of ϵ. Comparing this with the discussion in sect. 3.1 we see that increased ϵ implies a longer delay to initiate significant growth in x_B, but a more rapid final approach once in the neighbourhood of the steady state. Meanwhile sect. 4.3 suggests that, immediately subsequent to the delay time, the time required to transit to the neighbourhood of the steady state is ϵ independent. The question of how ϵ affects overall evolution time in the DS model is ambiguous, and depends on the precise definition one adopts for overall evolution time.

[7] Note that this choice is different from the value utilised in fig. 9 where a smaller value of x_{B0} value was chosen. This is due to the inclusion of the super-exponential growth formula in fig. 9, that formula only being valid when $x_B \ll x_0^{1/2}$.

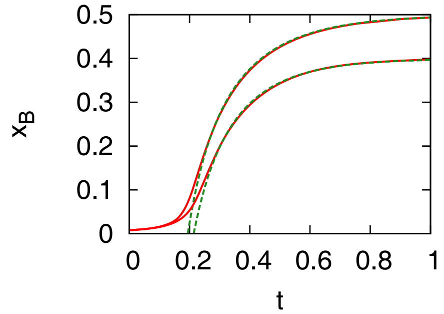

Fig. 10. Full numerical solution of x_B *vs.* t (solid line) plotted against the outer solution (dashed line): all quantities are in dimensionless form. The upper curves are for $\epsilon/\gamma_{\text{eq}} = 0$ and the lower curves are for $\epsilon/\gamma_{\text{eq}} = 1$.

4.8 Matching the intermediate solution onto the full numerical solution

Once $x_B \gg x_0^{1/2}$, the intermediate regime predicts $\dot{x}_B$ rising to a saturation value $\dot{x}_B^{\text{sat}}$, whereas in the full DS model, as x_B becomes significant compared to x_B^{final}, the value of $\dot{x}_B$ must fall again as x_B approaches steady state. Thus the saturation limit equation (22) of the intermediate regime solution must give way to an "outer" solution, which is obtained by substituting eq. (6) into eqs. (7) and (9). These outer solutions can be obtained numerically, the initial condition for the outer solution being $x_B^{\text{outer}} \to 0$ as $t \to t_{\text{delay}}$. As is evident from fig. 10, agreement between these outer solutions and the full numerical solutions of the DS model is good.

Note however that, whereas the outer solutions begin to grow at the saturation value $\dot{x}_B^{\text{sat}}$, the full numerical solutions never quite attain this value. The saturation velocity is only approached asymptotically in the regime $x_0^{1/2} \ll x_B \ll x_B^{\text{final}}$, a regime which is difficult to achieve in the full numerical solutions assuming realistic values of x_0 (we have chosen $x_0 = \frac{1}{128}$), for which $x_0^{1/2}$ and x_B^{final} differ by only a single order of magnitude. The concept of an intermediate regime provides a useful guide to understanding the full evolution of x_B *vs.* t, but we do not expect perfect agreement between the full solution and the intermediate asymptotics, an expectation which is borne out in practice.

5 Discussion and conclusions

We have analysed the Durand and Stone (DS) model [18] for relaxation of the T1 process in a foam.

The DS model is attractive on a number of levels: it is elegant enough to incorporate important surface rheological properties of foam films (Gibbs elasticity and surface viscosity), yet simple enough to be solved extremely inexpensively.

As well as addressing foam film geometry, the DS model also considers surfactant transport. It permits surfactant transport between adjacent films around the vertex connecting them, a transport mechanism which has not been considered by other studies [19–21, 23].

Permitting surfactant transport between films decouples the rate of increase of film length on a newly created film from the rate of stretch of material elements on that film, allowing the film not only to attain a much greater final length, but also to evolve more rapidly, compared to a case where surfactant transport between films is neglected.

The DS model however assumes a very specific amount of surfactant transport. Indeed the instantaneous surfactant concentration on the growing film can be deduced wholly in terms of the geometry, *i.e.* surfactant concentrations can be determined entirely in terms of instantaneous film lengths, without any reference to how those film lengths evolve with time. Moreover the surfactant concentration on the growing film is predicted to fall sharply with film length at short film lengths, but falls only very gradually at longer film lengths.

Whilst surfactant transport between adjacent films is a mechanism which is desirable to include in any T1 relaxation model, the question arises of whether the specific amount of transport assumed by DS is at the correct level. Experimentally of course one can observe film lengths during T1 relaxation, but surfactant concentrations are difficult to observe. Fortunately however, the surfactant transport mechanism assumed by DS implies a very definite signature for the evolution of the vertex postion following a T1: the vertex should have a quiescent delay period during which it moves comparatively little, then it exhibits a dramatic acceleration to reach a maximum saturation velocity, and subsequently its velocity decays as it reaches a final steady state length.

The experimental data presented by DS indicated a saturation velocity followed by a velocity decay towards a final steady length —the delay and acceleration phases were not however reported in the DS data. This does not a priori mean that the DS model is invalid. The delay and acceleration phases, which both occur when the vertex is comparatively short, may be easy to overlook experimentally: indeed the T1 might appear have begun with the saturation phase, whereas it in fact started somewhat earlier.

Relevant however is the study of Biance *et al.* [19] which made a careful experimental examination of the early stage growth of a film following a T1: this study observed early-time exponential growth (but never super-exponential growth) and therefore differs from the DS predictions. The reasons for that difference may be due to the fact that Biance *et al.*'s experiment was done on a fully 3-dimensional bubble cluster, whereas the DS model was derived for a 2-dimensional foam. If however experiments even on 2-dimensional systems do not display super-exponential early-time growth for the relevant film length, then new models for the amount of surfactant transport between adjacent films following a T1 need to be developed and tested. Indeed we have already commented (see the footnote in sect. 4.4) how a careful comparison between the observed experimental time scale for film growth and the growth times from model predictions can be used to estimate the extent of surfactant transport from film to film: this offers a promising avenue for future studies.

P. Grassia acknowledges support from CNRS visiting researcher contract number 240335 and thanks LPTM, CNRS UMR 8089 for hosting his visiting researcher stay. We acknowledge useful discussions with M. Durand.

Appendix A. Final state following a T1 with varying tensions in the shrinking film

In the main text (sect. 3) it was mentioned that tensions in the growing film and the shrinking films are unequal in the final state of the DS model, so the films do not all meet at equal angles. Indeed equal angles are only restored on longer time scales, associated with bringing fresh surfactant from the bulk of the film to the surface. Mathematically, in the DS model, the unequal tensions and unequal angles are consequences of allowing the tension in the growing film to evolve, but assuming that the tensions in the shrinking films remain fixed. Such an assumption seems reasonable whilst the growing film is much shorter than its neighbours, but that is not the case in the final state.

In this appendix, the consequences of relaxing the assumption of fixed tensions on the shrinking film are considered, particularly with regard to how they relate to the final state of the T1 process. We will show that, in a final state with physically plausible film tensions, unequal film meeting angles persist, with (as in the DS model) the size of the inequality growing with $\epsilon/\gamma_{\mathrm{eq}}$. It is not however necessary to invoke the DS model with its assumption of fixed equilibrium tensions on the shrinking films to explain unequal film meeting angles.

When one considers that the tension in a shrinking film differs from γ_{eq}, the question arises whether both surfaces of the shrinking film have the same tension. In fact it seems reasonable to suppose that the tensions on either surface of the shrinking film actually differ, as will now be explained.

As is evident in fig. 2 one surface of the shrinking film connects directly to the surface of the growing film. Although these connected surfaces exchange surfactant between themselves, the total amount of surfactant on them is conserved, because the process of bringing fresh surfactant from the bulk is assumed to occur on time scales much longer than those of present interest. To achieve a steady state configuration, these connected surfaces ought to attain the same surfactant concentration: this follows because any inequity in surfactant concentration where the surfaces join would drive Marangoni flows.

On the other hand, the remaining surface of the shrinking film connects only to a reflected copy of itself, and does not connect to the growing film. It seems reasonable to

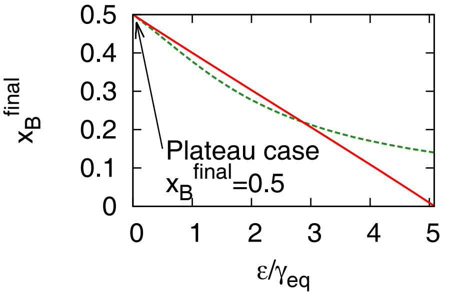

Fig. 11. The final state $x_B^{\rm final}$ *vs.* $\epsilon/\gamma_{\rm eq}$ computed by the DS model (solid line) and by the alternative approach presented in appendix A (dashed line).

suppose that the total amount of surfactant on this side of the shrinking film is conserved: any non-conservation would require transport of surfactant from the film into the bulk, which to be consistent with previous assumptions, should be a slow process.

Suppose the system achieves a final steady configuration $x_B^{\rm final}$. The final surfactant concentrations on the growing film and on the connected surface of the shrinking film will be $\Gamma_{\rm eq} L_c/(x_B^{\rm final} + L(x_B^{\rm final}))$ where we need to use eqs. (1) and (3). The final surfactant concentration on the remaining surface of the shrinking film will be $\Gamma_{\rm eq} L(x_0)/L(x_B^{\rm final})$.

Unequal surfactant concentrations on either side of the shrinking film imply unequal film tensions on either side. It is therefore the inequity between the tension on either side of the shrinking film (rather than, as in the DS model, the assumption of a persistent tension difference between the growing and shrinking films) which produces unequal film meeting angles here. Indeed force balance now demands (*in lieu* of eq. (10))

$$\gamma_{\rm eq} - \epsilon \log \frac{L_c}{(x_B^{\rm final} + L(x_B^{\rm final}))} = \cos\alpha(x_B^{\rm final}) \times \left(2\gamma_{\rm eq} - \epsilon \log \frac{L_c}{(x_B^{\rm final} + L(x_B^{\rm final}))} - \epsilon \log \frac{L(x_0)}{L(x_B^{\rm final})} \right), \tag{A.1}$$

where eqs. (1)–(2) must be used.

Solutions of eq. (A.1) for $x_B^{\rm final}$ can be readily obtained and are found to be insensitive to the parameter x_0 provided $x_0 \ll 1$ is small. Thus $x_B^{\rm final}$ is primarily a function of $\epsilon/\gamma_{\rm eq}$.

Results are plotted in fig. 11 where they are compared against the values obtained by the DS model. Clearly there is qualitative agreement between the two sets of predictions with $x_B^{\rm final}$ decreasing as $\epsilon/\gamma_{\rm eq}$ increases. Moreover up to $\epsilon/\gamma_{\rm eq}$ values of around three, there is even good quantitative agreement between the predictions. Since (as mentioned in the main text) typical experimental $\epsilon/\gamma_{\rm eq}$ values are likely to be considerably smaller than three, looking at final states alone is not an exceedingly rigorous experimental test of the DS model compared to alternative plausible hypotheses for the extent of surfactant transport between films. A far more robust test of the DS model therefore is that proposed in the main text which considers the early time temporal evolution of the length of the growing film.

In this appendix we have presented a self-consistent theory for the final surfactant concentration on films following a T1, where we permit the final concentration in the shrinking film to differ from the initial value. The theory relied on the fact that, in the final state, the surfactant concentration on the growing film and on the shrinking film surface to which it is connected, must be the same. These concentrations should not however be the same at all times leading up to the final state, meaning that the theory is not sufficient to compute the time evolution of x_B for a case where the instantaneous concentration in the shrinking film is permitted to differ from its initial value. In order to achieve that, one would need a relation between the instantaneous state of the system and the instantaneous rate at which the growing film receives surfactant from that surface of the shrinking film to which it is connected. Any generalisation of the DS model to the case of variable-concentration shrinking films would require formulation of such a relation.

Appendix B. Obtaining the values of x_{B0} and t_0

In the main text (sects. 4.2 and 4.6), we presented a number of asymptotic formulae for x_B *vs.* t parameterised in terms of two quantities denoted x_{B0} and t_0. In those sections, x_{B0} was an arbitrarily chosen film length (much greater than initial film length x_0, but still much smaller than unity), and t_0 was the time corresponding to $x_B = x_{B0}$. We stated in the main text that, for any chosen x_{B0}, the required value t_0 could be obtained numerically. Analytic estimates of t_0 are however also available, as we now explain.

Provided x_B is small, eqs. (7)–(8) become

$$(\sqrt{3}-1)\gamma_{\rm eq} + \epsilon \log(\Gamma/\Gamma_{\rm eq}) + \mu ({\rm d}/{\rm d}t) \left(\log(\Gamma/\Gamma_{\rm eq})\right) \approx 0. \tag{B.1}$$

Without loss of generality we assume (as adopted in the main text) units for which $\gamma_{\rm eq} = 1$, $\Gamma_{\rm eq} = 1$ and $\mu = 1$. The solution for Γ is

$$\Gamma \approx \exp\left(-\frac{(\sqrt{3}-1)}{\epsilon} \left(1 - \exp(-\epsilon t)\right) \right). \tag{B.2}$$

Equation (4) now determines x_B once Γ is known, where L and L_c in that equation are given by eqs. (1) and (3) respectively. If $x_0 \ll 1$ and also $x_B \ll 1$, we can Taylor expand the formulae for L_c and L, to obtain eq. (5). This rearranges to

$$\frac{x_B}{x_0} \approx \frac{\left(1 - \frac{\sqrt{3}}{2}\right)}{\left(\Gamma - \frac{\sqrt{3}}{2}\right)}. \tag{B.3}$$

If we set $x_B = x_{B0}$ in this equation with x_{B0} satisfying $x_{B0} \gg x_0$ (*e.g.* with an arbitrary choice such as $x_{B0} \equiv$

$x_0^{1/2}$ as in sect. 4.6), then at leading order t_0 can be obtained[8] by setting $\Gamma \approx \frac{\sqrt{3}}{2}$ in eq. (B.2). Hence

$$t_0 \approx \frac{1}{\epsilon} \log\left(\frac{1}{\left(1-\frac{\epsilon \log(2/\sqrt{3})}{(\sqrt{3}-1)}\right)}\right) \approx \frac{1}{\epsilon}\log\left(\frac{1}{2x_B^{\mathrm{final}}}\right), \quad \text{(B.4)}$$

where eq. (11) has been used to define x_B^{final}. Moreover eq. (23) (again with x_{B0} chosen to equal $x_0^{1/2}$ say) then indicates that t_0 matches the so called delay time t_{delay} to within a relative error of $O(x_0^{1/2})$. Equation (B.4) describes a function which grows with ϵ, following closely the same behaviour as t_{delay} exhibits in fig. 6.

References

1. A.M. Kraynik, Annu. Rev. Fluid Mech. **20**, 325 (1988).
2. D. Weaire, S. Hutzler, *The Physics of Foams* (Clarendon Press, Oxford, 1999).
3. R. Höhler, S. Cohen-Addad, J. Phys.: Condens. Matter **17**, R1041 (2005).
4. D. Weaire, Curr. Opin. Colloid Interface Sci. **13**, 171 (2008).
5. D.A. Reinelt, A.M. Kraynik, J. Rheol. **44**, 453 (2000).
6. Y.H. Wang, K. Krishan, M. Dennin, Phys. Rev. E **73**, 031401 (2006).
7. Y.H. Wang, K. Krishan, M. Dennin, Phys. Rev. E **74**, 041405 (2006).
8. G. Katgert, M.E. Möbius, M. van Hecke, Phys. Rev. Lett. **101**, 058301 (2008).
9. W. Drenckhan, S.J. Cox, G. Delaney, H. Holste, D. Weaire, N. Kern, Colloids Surf. A, Physicochem. Engg Aspects **263**, 52 (2005).
10. H.M. Princen, J. Colloid Interface Sci. **91**, 160 (1983).
11. A.D. Gopal, D.J. Durian, Phys. Rev. Lett. **75**, 2610 (1995).
12. T. Okuzono, K. Kawasaki, Phys. Rev. E **51**, 1246 (1995).
13. A.D. Gopal, D.J. Durian, J. Colloid Interface Sci. **213**, 169 (1999).
14. R.A. Leonard, R. Lemlich, AIChE J. **11**, 18 (1965).
15. M. Durand, G. Martinoty, D. Langevin, Phys. Rev. E **60**, R6307 (1999).
16. J. Lucassen, in *Anionic Surfactants: Physical Chemistry of Surfactant Action*, edited by E.H. Lucassen-Reynders, chapt. 6 (Marcel Dekker, Inc., New York, Basel, 1981) pp. 217–265.
17. K. Małysa, R. Miller, K. Lunkenheimer, Colloids Surf. **53**, 47 (1991).
18. M. Durand, H.A. Stone, Phys. Rev. Lett. **97**, 226101 (2006).
19. A.-L. Biance, S. Cohen-Addad, R. Höhler, Soft Matter **5**, 4672 (2009).
20. I. Cantat, Soft Matter **7**, 448 (2011).
21. P. Grassia, B. Embley, C. Oguey, J. Rheol. **56**, 501 (2012).
22. N.D. Denkov, S. Tcholakova, K. Golemanov, K.P. Ananthpadmanabhan, A. Lips, Soft Matter **5**, 3389 (2009).
23. B. Embley, P. Grassia, Colloids Surf. A: Physicochem. Engg Aspects **382**, 8 (2011). Special Issue: A collection of papers from the 8th EUFOAM conference and the meetings of COST Actions D43 and P21.

[8] At the next order, the required target value of Γ would be $\frac{\sqrt{3}}{2} + (1-\frac{\sqrt{3}}{2})x_0 x_{B0}^{-1}$ (typically with $x_{B0} = x_0^{1/2}$), and this would lead to a prediction

$$t_0 \approx \frac{1}{\epsilon}\log\left(\frac{1}{\left(1-\frac{\epsilon\log(2/\sqrt{3})}{(\sqrt{3}-1)}\right)}\right) - \frac{\left(1-\frac{\sqrt{3}}{2}\right) x_0 x_{B0}^{-1}}{\frac{\sqrt{3}}{2}(\sqrt{3}-1)\left(1-\frac{\epsilon \log\frac{2}{\sqrt{3}}}{(\sqrt{3}-1)}\right)}.$$

Employing eqs. (11) and (17) to define quantities x_B^{final} and $\dot{x}_B^{\mathrm{sat}}$, and using the definition of the numerical constant χ from sect. 4.6, reveals

$$t_0 \approx \frac{1}{\epsilon}\log\left(\frac{1}{2x_B^{\mathrm{final}}}\right) - \frac{\chi x_0}{\dot{x}_B^{\mathrm{sat}} x_{B0}},$$

and thence via eq. (23)

$$t_{\mathrm{delay}} \approx \frac{1}{\epsilon}\log\left(\frac{1}{2x_B^{\mathrm{final}}}\right) - \frac{x_{B0}}{\dot{x}_B^{\mathrm{sat}}}.$$